JCTC Journal of Chemical Theory and Computation

Article

pubs.acs.org/JCTC

# A Quasidegenerate Second-Order Perturbation Theory Approximation to RAS-*n*SF for Excited States and Strong Correlations

Nicholas J. Mayhall, Matthew Goldey, and Martin Head-Gordon*

Kenneth S. Pitzer Center for Theoretical Chemistry, Department of Chemistry, University of California, Berkeley, Berkeley, California 94720, United States

Chemical Sciences Division, Lawrence Berkeley National Laboratory, Berkeley, California 94720, United States

Supporting Information

**ABSTRACT:** We present a modification of the recently developed Restricted Active Space with *n* Spin Flips method (RAS-*n*SF), which provides significant efficiency advantages. In the RAS-*n*SF configuration interaction wave function, an arbitrary number of spin-flips are performed within an orbital active space (often simply the singly occupied orbitals), with state-specific orbital relaxation being described by single excitations into and out of the active space (termed hole and particle states, respectively). As the number of hole and particle states dominates the cost of the calculation, we present an attractive simplification in which the orbital relaxation effects (via hole and particle states) are treated perturbatively rather than variationally. The physical justification for this simplification stems from the spin-flip methodology itself, which suggests that the underlying molecular orbitals (high-spin ROHF) are capable of providing a decent description of the target (spin-flipped) electronic states. The current approach termed SF-CAS(h,p)$_n$ (Spin-Flip Complete Active-Space with perturbative Hole and Particle states) yields spin-pure energies and eigenfunctions due to the spin-free formulation. A description of the theory is presented, and a number of numerical examples are investigated to determine the accuracy of the approximation. Computational speedups of over 100 times were demonstrated on a 254 electron, 358 basis function calculation on a Cu(II) porphyrin derivatized with a verdazyl group.

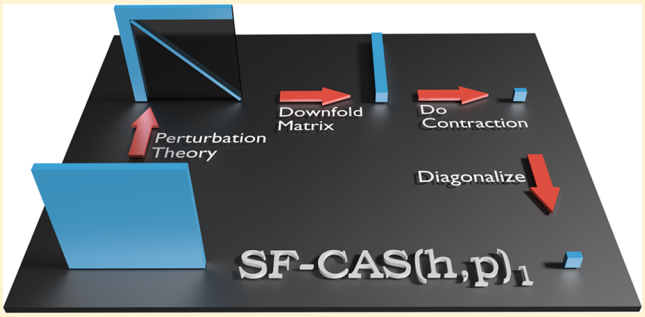


## I. INTRODUCTION

In electronic structure theory, ab initio approaches to modeling the electrons in a molecular system provide computational chemists with a prescription for obtaining arbitrarily accurate results, *in principle*. However, without making assumptions about the system at hand, the computational complexity increases exponentially with the size of the system. For many stable molecules in their equilibrium geometry, it is reasonable to assume that a single Slater determinant can provide a qualitatively correct description of the electronic wave function. This is an effective approximation when all the electrons are tied up in chemical bonds, and many-body corrections (such as many-body perturbation theory (MBPT) or coupled cluster theory (CC))[1−4] can be added to obtain quantitatively accurate results.

For systems with unpaired electrons or very low-lying excited states, a single Slater determinant is no longer an adequate approximation to the ground state nor an effective reference state for MBPT or CC approximations. This interaction among low-lying configurations is somewhat ambiguously termed "static correlation" or "strong correlation" and makes even a qualitatively correct description difficult. The electronic characteristics which give rise to static correlation are, in fact, the same characteristics which lead to chemical reactivity (small HOMO−LUMO gap, unpaired electrons). It is, therefore, not surprising that investigations into photochemistry or catalysis are often hindered by the availability of computationally efficient methods which describe static correlation.

Many directions have been explored to treat static correlation, each with varying utility and accuracy. Of these, CASSCF (complete active space self-consistent field) has been the most commonly used approach to obtain a qualitatively correct reference state for multireference systems.[5] Due to the high computational cost and practical challenges in using CASSCF, new approaches to this problem are also being pursued.[6−11] Most notably, perhaps, is the density matrix renormalization group (DMRG) approach, which has been shown to exhibit polynomial rather than exponential scaling, enabling computations of larger active spaces.[6,12,13] Many-body methods can then be applied to the resulting wave function to describe dynamical correlation (CASPT2), which is required for quantitative accuracy.[14] These methods, however, are burdened by difficult orbital convergence, the need for state-averaging, and the intruder state problem.

A promising single-reference alternative approach is the "spin-flip" framework introduced by Krylov and co-workers.[15−18] Spin-

**Received:** October 15, 2013
**Published:** December 20, 2013

flip methods are based on the fact that in many cases where static correlation plays a role (bond-breaking, biradical electronic states), a low-lying, high-spin, excited state exists which is single determinantal. The spin-flip approach takes this high spin Hartree−Fock determinant as the reference state. The states with the desired $M_s$ value (i.e., the ground state) are then described by a linear combination of spin-flipping excitations ($\alpha \rightarrow \beta$). By placing all strongly correlated electrons into orbitals with the same spin function, the high-spin reference can no longer couple to the low-lying excited states (since they have a different number of $\alpha$ and $\beta$ electrons), thus providing a valid single reference determinant. Spin-flip, thus, provides a genuine single reference solution to a multireference problem, in which all the CI determinants are treated on an equal footing.

The simplest realization of the spin-flip model is SF-CIS (spin-flip configuration interaction singles) where only single spin-flipping operators act on a high-spin triplet reference.[19] This has the ability to provide qualitatively correct descriptions of single bond breaking and open-shell singlet states (antiferromagnetic coupling) of biradicaloid molecules. Many spin-flip methods have been implemented which also account for dynamic correlation via CI,[16] CC,[20] DFT,[21−23] and MBPT,[19] providing quantitatively accurate results for appropriate systems.

Despite the success of the spin-flip approach to studying spin-coupled systems, a few shortcomings were noticed early on,[24] such as the problem with spin-contamination in the resulting low-spin wave function. For instance, SF-CIS does not yield pure spin eigenfunctions, even if the underlying reference wave function has no spin contamination (such as with a restricted open shell Hartree−Fock reference (ROHF)). This is due to the spin asymmetry of the reference (only using the $M_s = 1$ component of the triplet state) and the resulting absence of certain double and triple excitations which provide the proper spin complementing Slater determinants required to form a configuration state function. This also results in an artificial energy gap between the $M_s = 1/-1$ and $M_s = 0$ components of the triplet state. To address this problem, Sears et al. developed spin-complete spin-flip CIS (SC-SF-CIS),[24] which produced pure spin states with improved results. The SC-SF-CIS method was later generalized by including more excited configurations in the SF-XCIS method.[25]

In order to extend spin-pure treatments of spin-flip CI to a larger number of spin-flips, the RAS-*n*SF method was introduced by Casanova et al.[26−28] RAS-*n*SF is defined using high spin ROHF orbitals which are grouped into three subspaces, RAS I, RAS II, and RAS III. This subspace grouping is illustrated in Figure 1, and the RAS-*n*SF wave function is defined as

$$\Psi_s^{\mathrm{RAS}} = \sum_A c_A^s \varphi_A + \sum_h c_h^s \varphi_h + \sum_p c_p^s \varphi_p \tag{1}$$

where $\phi_A$ are the set of CAS determinants (full CI in RAS II), and $\phi_h$ and $\phi_p$ are the determinants from RAS I → II (hole) excitations and RAS II → III (particle) excitations, respectively. For a fixed number of spin-flips, increasing the system size does not affect the number of CAS determinants ($\phi_A$), while the hole and particle determinants ($\phi_h$, $\phi_p$) increase only linearly with system size. One of the prominent advantages of the spin-flip approach is that orbital optimization is not being performed on the multideterminantal wave function; RAS-*n*SF is simply a CI expansion using high-spin orbitals.

RAS-*n*SF can be thought of as a many-spin-flip generalization of the SF-XCIS approach, in which direct hole → particle excitations are neglected. Alternatively, one can think of RAS-*n*SF as an extended CAS-CI method where the CAS-CI wave function is of the spin-flip type: SF-CAS-CI. The increased flexibility of the RAS-*n*SF wave function compared to the SF-CAS-CI wave function is obtained by including the hole and particle excitations, which provide two benefits:

- state-specific orbital relaxation of all SF-CAS-CI states
- access to certain singly excited electronic states not present in the SF-CAS-CI wave function

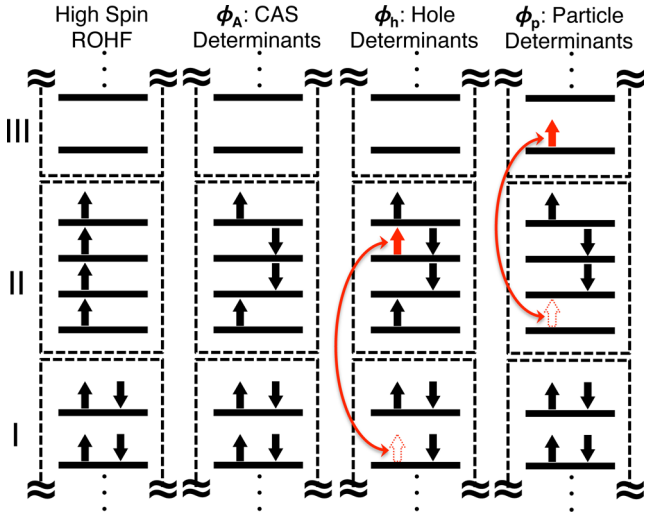


**Figure 1.** Schematic representation of the classes of determinants in the RAS(4,4)-2SF wave function expansion.

The hole and particle excitations are clearly necessary if one is aiming to describe an electronic state that is predominately of hole or particle character. However, for the more common scenario in which one is interested in states primarily described by excitations within the active space, then it is the orbital relaxation effect that is relevant. Because the high-spin HF orbitals are believed to be satisfactory (which is the foundation of the spin-flip framework), one might expect the orbital relaxation effects of the SF-CAS-CI states to be rather small and thus able to be described by perturbation theory. In this paper, we consider this possibility by developing a quasidegenerate perturbation theory correction to SF-CAS-CI, which aims to reproduce the full RAS-*n*SF results but at significantly reduced computational effort.

## II. THEORY

As part of a series of articles on perturbation theory,[29−31] Löwdin developed a general partitioning technique which recasts the Schrödinger equation into a convenient form for employing various approximations.[32−34] By partitioning the CI secular equation into a small primary space ($A$) and a larger external space ($X$)

$$\begin{pmatrix} \mathbf{H}_{AA} & \mathbf{H}_{AX} \\ \mathbf{H}_{XA} & \mathbf{H}_{XX} \end{pmatrix} \begin{pmatrix} \mathbf{C}_A \\ \mathbf{C}_X \end{pmatrix} = E_s \begin{pmatrix} \mathbf{C}_A \\ \mathbf{C}_X \end{pmatrix} \tag{2}$$

one can regroup the equations to obtain the exact energy for state $s$ by diagonalizing an energy-dependent effective Hamiltonian of only $A \times A$ dimension.

$$\mathcal{H}_{AA,s}\mathbf{C}_A = E_s\mathbf{C}_A \tag{3}$$

where


dx.doi.org/10.1021/ct400898p | J. Chem. Theory Comput. 2014, 10, 589−599

$$\mathcal{H}_{AA,s} = \mathbf{H}_{AA} + \mathbf{H}_{AX}[E_s - \mathbf{H}_{XX}]^{-1}\mathbf{H}_{XA} \tag{4}$$

As this is completely equivalent to the full CI problem, eq 4 still requires the diagonalization of the $\mathbf{H}_{XX}$ block of the Hamiltonian. Further, eq 3 must now be solved iteratively for each eigenvalue due to the energy dependence and state-specific nature of the effective Hamiltonian. Computational simplification occurs when one chooses an approximation to $\mathbf{H}_{XX}$, such that the formation of the denominator becomes trivial to compute. Further simplifications may also be invoked to remove the energy dependence from the effective Hamiltonian.

In the present method, we define the $A$ space to contain all determinants in the SF-CAS-CI wave function and the $X$ space to contain the hole and particle excitations. This is different than other approaches which use perturbation theory to help account for the orbital relaxation to improve the minimal active-space CI,[35] as the spin-flip approach circumvents the orbital optimization entirely.

We define our zeroth order Hamiltonian as

$$\mathbf{H} = \mathbf{H}^{(0)} + \lambda\mathbf{H}^{(1)} \tag{5}$$

$$\mathbf{H}^{(0)} = \begin{pmatrix} \hat{H} & 0 \\ 0 & \hat{F} + \langle|\hat{V}|\rangle + \eta \end{pmatrix} \tag{6}$$

$$\mathbf{H}^{(1)} = \begin{pmatrix} 0 & \hat{H} \\ \hat{H} & \hat{V} - \langle|\hat{V}|\rangle - \eta \end{pmatrix} \tag{7}$$

where $\hat{H}$, $\hat{F}$, and $\hat{V}$ are the Hamiltonian, Fock operator, and fluctuation potential, respectively. The reference state, $|\rangle$, is taken to be the zeroth-order ground-state SF-CAS-CI wave function,[81] and the scalar quantity, $\eta$, is an arbitrary level-shift chosen to increase the energy of the perturbing levels in the zeroth order Hamitonian. At zeroth order, the exact Hamiltonian exists only in the $A$ space, with the one electron Fock operator, $\hat{F}$, describing the zeroth order energy of the determinants in the $X$ space.

The level shift, $\eta$, can alternatively be interpreted as a penalty function which damps large amplitudes in the perturbative space, stabilizing the perturbative expansion. Using indices $a$ and $b$ to represent SF-CAS determinants ($A$ space), indices $x$ and $y$ to represent hole and particle determinants ($X$ space), and indices $p$ and $q$ to represent general determinants ($A \cup X$ space), the Lagrangian for this system is

$$\mathcal{L} = \sum_{pq} c_p H_{pq} c_q \quad -E\sum_p (c_p^2 - 1) + \eta\sum_x c_x^2 \tag{8}$$

Making this stationary with respect to the $A$ and $X$ space coefficients

$$\frac{\partial\mathcal{L}}{\partial c_a} = \sum_b H_{ab}c_b + \sum_y H_{ay}c_y - Ec_a = 0 \tag{9}$$

$$\frac{\partial\mathcal{L}}{\partial c_x} = \sum_b H_{xb}c_b + \sum_y H_{xy}c_y - Ec_x + \eta c_x = 0 \tag{10}$$

leads to a modified effective Hamiltonian with a level shift in the denominator:

$$\mathcal{H}_{ab,s} = H_{ab} + \sum_x H_{ax}[E_s - H_{xx} - \eta]^{-1}H_{xb} \tag{11}$$

Larger values of $\eta$ will consequently yield smaller perturbative corrections.

Substituting with eq 5, we can expand the effective Hamiltonian in eq 11, $H_{ab,s}$, in order of the perturbation.

$$\mathcal{H}^{(2)}_{ab,s} = H_{ab} + \sum_x \frac{H_{ax}H_{xb}}{E_s - F_x - V_0^{(0)} - \eta} \tag{12}$$

Diagonalization of the zeroth-order Hamiltonian yields the SF-CAS-CI energy and wave function. The first correction shows up at second order and includes only the diagonal of the $X$ space in the denominator (by choosing an appropriate $\hat{F}$ which is diagonal in the determinant basis), making the denominator trivial to compute.

This can lead directly to a *nondegenerate* second order perturbative correction, referred to here as SF-CAS(h,p), by taking the expectation value of the effective Hamiltonian (eq 12) in the zeroth-order eigenvector basis.

$$E_s^{\mathrm{SF-CAS(h,p)}} = \sum_{ab} c_{a,s}^{(0)}\mathcal{H}^{(2)}_{ab,s}c_{b,s}^{(0)} \tag{13}$$

If an accidental degeneracy arises in the zeroth order problem, the perturbation is not well-defined, as any nonzero Hamiltonian coupling introduced by the perturbation would result in an infinite first-order correction to the two degenerate states. This requires one to variationally remix the states in the presence of the perturbation, via a *quasidegenerate* perturbation theory (QDPT). To do this in a well-defined manner, one can choose to remix all of the states after adding the perturbation into the effective Hamiltonian, i.e., a "perturb-then-diagonalize" approach.

However, as indicated by the state index ($s$) on $\mathcal{H}^{(2)}_{ab,s}$, the effective Hamiltonian has a state dependence, which (if not removed) makes it necessary to form a separate state-specific effective Hamiltonian for each state being solved. To remove the state dependence, we write the denominator as

$$D^{(0)}_{x,s} = E_s - F_x - V_0^{(0)} - \eta \tag{14}$$

$$= \omega_s + E_0^{(0)} - F_x - V_0^{(0)} - \eta \tag{15}$$

$$= \omega_s - \omega_x^{(0)} - \eta \tag{16}$$

where $\omega_s$ is the excitation energy of the state of interest, $s$, and

$$\omega_x^{(0)} = \langle X|\hat{F}|X\rangle - \langle|\hat{F}|\rangle \tag{17}$$

$$= \sum_{i\in|\varphi_x\rangle}\varepsilon_i - \sum_a\sum_{i\in|\varphi_a\rangle}(c_{a,0}^{(0)})^2\varepsilon_i \tag{18}$$

As was done in the CIS($D_0$) method,[36−38] expanding the denominator in orders of $\omega_s/(\omega_x^{(0)} + \eta)$ yields an expansion that, when truncated at either the zeroth or first order, removes the state dependence of $\mathcal{H}^{(2)}_{ab,s}$.

$$\frac{1}{\omega_s - \omega_x^{(0)} - \eta} = -\frac{1}{\omega_x^{(0)} + \eta} \tag{19}$$

$$-\frac{\omega_s}{(\omega_x^{(0)} + \eta)^2} + \ldots \tag{20}$$

This expansion is rapidly convergent provided that the state of interest, $s$, is close in energy to the ground state relative to the external space determinants. As we are typically interested in the few lowest energy states, this should generally not be a problem.

Truncation of the denominator at zeroth or first order defines the SF-CAS(h,p)$_0$ and SF-CAS(h,p)$_1$ methods, respectively. In


dx.doi.org/10.1021/ct400898p | J. Chem. Theory Comput. 2014, 10, 589−599

both cases, the different state energies are obtained by a single diagonalization of a state-independent effective Hamiltonian, making this a multistate theory. However, in the case of SF-CAS(h,p)$_1$, the presence of $\omega_s$ in the numerator requires one to solve a generalized eigenvalue equation.

$$\mathcal{H}^{(2)}\mathbf{C} = \mathcal{S}\mathbf{C}E \tag{21}$$

**A. SF-CAS(h,p)$_0$.** The SF-CAS(h,p)$_0$ method offers the simplest QDPT correction. Here, the denominator is simply orbital energy differences, and the metric, $\mathcal{S}_{AA}$, is the identity matrix, $\mathbf{I}_{AA}$. The effective Hamiltonian to diagonalize is

$$\mathcal{H}^{(2)}_{ab} = H_{ab} - \sum_x \frac{H_{ax}H_{xb}}{\omega_x^{(0)} + \eta} \tag{22}$$

**B. SF-CAS(h,p)$_1$.** The SF-CAS(h,p)$_1$ method linearly corrects for the loss of state specificity in the effective Hamiltonian. Keeping only the first two terms of the expansion in eq 19 and rearranging yields the following Hamiltonian and metric:

$$\mathcal{H}^{(2)}_{ab} = H_{ab} - \sum_x \frac{H_{ax}H_{xb}}{\omega_x^{(0)} + \eta} + E_0^{(0)} \sum_x \frac{H_{ax}H_{xb}}{(\omega_x^{(0)} + \eta)^2} \tag{23}$$

$$\mathcal{S}_{ab} = 1 + \sum_x \frac{H_{ax}H_{xb}}{(\omega_x^{(0)} + \eta)^2} \tag{24}$$

It is useful to compare the current method to other related theoretical approaches in the literature. Of particular relevance is the difference dedicated configuration interaction (DDCI) method of Malrieu and co-workers,[39,40] which has been successfully used for the computation of spin-state energy gaps.[35,41−45] In DDCI, a variational CI space is selected by including all determinants which couple to a model determinant space (CAS) at second-order perturbation theory. This space was then decomposed into a hierarchy CASCI, DDCI1, DDCI2, and DDCI, which differs based on the number of external indices on the excited determinants defining the variational space.[41] The RAS-*n*SF method itself can be thought of as a spin-flip DDCI1 method, taking the singly occupied orbitals as the model space. So while the SF-CAS(h,p)$_n$ approach was motivated as a perturbative approximation to a variational CI problem, the DDCI method was motivated as a variational extension of a perturbative theory. Similar to our current method, Barone et al. have used Löwdin partitioning to increase efficiency in computing singlet−triplet gaps via DDCI.[43,45,46] This was done by partitioning a spin-coupled system into local fragments to reduce the size of the CI space and including part of the determinantal space variationally and the rest perturbatively. Our approach falls within the spin-flip group of methods, thus leaning on the reliability of the high-spin orbitals for providing a single configuration reference wave function. We have also targeted a low cost approach by exclusively taking the SF-CAS as the zeroth order wave function and including significantly fewer determinants in the perturbation.

**C. Choice of $\hat{F}$.** Finally, to fully define the current methodology, attention must be paid to the form of the Fock operator chosen in the $X$ subspace of the zeroth order Hamiltonian in eq 6. Our principle motivation in choosing a zeroth order Hamiltonian was to obtain a matrix which was already diagonal in the $\mathbf{H}^{(0)}_{XX}$ block. However, the ROHF Fock matrix is not actually diagonal in the determinant basis, due to the absence of variational parameters which would break spin symmetry. This requires one to select only parts of the Fock matrix to keep in the zeroth-order Hamiltonian, pushing the rest off to the perturbation.

In the context of ROHF-based MP2, it is well-known that the form of the ROHF Fock matrix leads to some degree of ambiguity in the perturbation,[47−55] and the current method is no exception. To ensure a spin-pure treatment of our perturbation, we construct a spin-free effective Fock matrix, which when diagonalized, leaves the energy of the high-spin ROHF wave function unchanged. This requires the off-diagonal blocks (in the MO basis) coupling the **D** and **S** blocks and the **S** and **V** blocks to come from the $\beta$ and $\alpha$ Fock matrices, respectively. Although the off-diagonal blocks are fixed by the HF stationary conditions, the diagonal blocks can be arbitrarily chosen.

One obvious choice would be to use the orbitals employed in the RO-based MP2 method, OPT1, which is spin-pure and has the same orbital invariant properties as the underlying ROHF wave function.[50] This approach takes the average of the $\alpha$ and $\beta$ Fock matrices for the diagonal blocks. We have chosen to use these orbitals, which diagonalize the following effective Fock matrix:

$$\mathbf{F} = \begin{pmatrix} \mathbf{F}^{\text{avg}} & \mathbf{F}^{\beta} & \mathbf{F}^{\text{avg}} \\ \mathbf{F}^{\beta} & \mathbf{F}^{\text{avg}} & \mathbf{F}^{\alpha} \\ \mathbf{F}^{\text{avg}} & \mathbf{F}^{\alpha} & \mathbf{F}^{\text{avg}} \end{pmatrix} \tag{25}$$

The potential drawback to choosing this zeroth order partitioning is that the orbital energies in the singly occupied block (the magnetic orbitals) are understood to correspond to the average of ionization potentials and electron affinities.[82] This diminishes the reliability of the Fock operator in estimating the energies of the perturbing states. However, by choosing a suitable value for the level-shift parameter, $\eta$, the accuracy of the PT correction can be improved while retaining properties which are very important for the current problem, namely spin-purity and orbital invariance.

**D. Implementation.** Because the methods presented here contain the full CI wave function in the active space, the computational complexity will always increase factorially with the size of the active space. However, with small active spaces, the computational bottlenecks will actually occur when computing the two-electron integrals. It is clear that these two limiting cases might have different optimal implementations, and we have developed the current code to target the small active space scenario. Note that in the following, any statements regarding computational scaling should be understood to mean increasing the molecular system or basis set size while holding the size of the active space constant.

In the SF-CAS(h,p)$_n$ methods, the only matrices to be diagonalized are of the smaller zeroth-order dimension. Therefore, we directly diagonalize both the $H_{ab}$ and $H^{(2)}_{ab}$ matrices. While our implementation is indeed general, the fact that we use a direct diagonalization (rather than a matrix-free Davidson solver) means that we are limited in practice in the size of active spaces allowed, which happens to be around four spin-flips.

Exploiting the sparsity of the Hamiltonian matrices, we use the $\alpha,\beta$-string techniques of Ruedenburg[56] with varying active space occupations to index our CI determinant space.

Our code proceeds by performing the following sequence of steps:.

1. Compute ROHF energy and orbitals
2. Obtain new spin-free orbitals from effective Fock matrix
3. Compute and store in memory $\hat{J}_{\mu\nu}$,$\hat{K}_{\mu\nu}$: $O(N^3)$


dx.doi.org/10.1021/ct400898p | J. Chem. Theory Comput. 2014, 10, 589−599

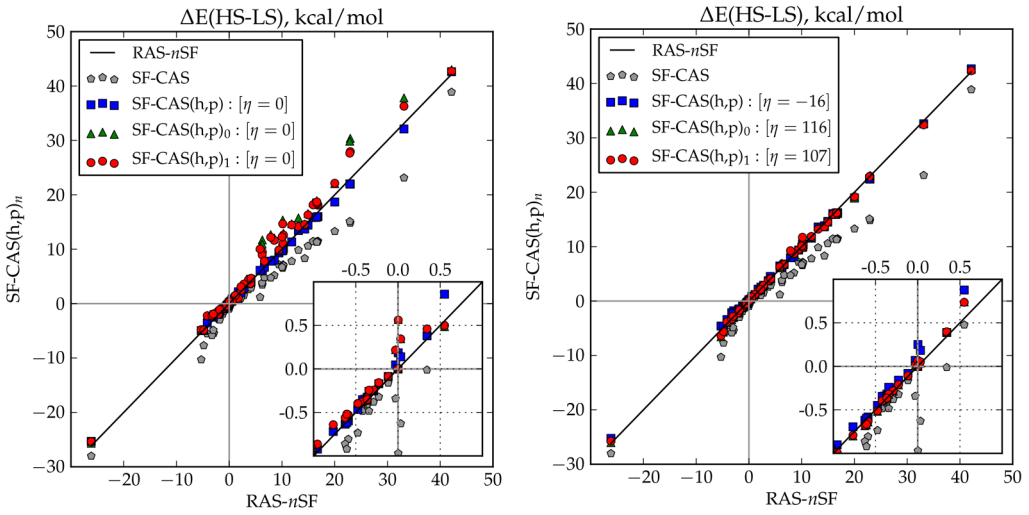


**Figure 2.** High spin−low spin state energy gaps. Perturbative results ($y$ axis) plotted against RAS-$n$SF ($x$ axis) results. Black line: RAS-$n$SF. Gray pentagons: SF-CAS. Blue squares: SF-CAS(h,p). Green triangles: SF-CAS(h,p)$_0$. Red circles: SF-CAS(h,p)$_1$. Data below (above) the black diagonal line indicates under(over)-estimation of low-spin energy relative to the high-spin state. Energy gaps with the wrong sign show up in +,− quadrants. Units in kcal/mol.

4. Compute and store in memory $(pq|rs)$, $(Pq|rs)$ via RI approximation: $O(N^3)$
5. Form and diagonalize $H_{ab}$: $O(N^0)$
6. Build $\mathscr{H}^{(2)}$: $O(N^1)$

- Find memory-allowed batches of the contraction index $x$ for $\sum_x H_{ax}D_xH_{bx}$
- Loop over $x_i$-batches (openMP[57] parallelized): $O(N^1)$
- Form blocks of $\mathbf{H}^i_{AX}$ and $\mathbf{D}^i_X$ for each batch $i$
- Increment $\mathcal{H}^{(2)} += \mathbf{H}^i_{AX}(\mathbf{D}^i_X \bigcirc \mathbf{H}^i_{XA})$
- Diagonalize $\mathcal{H}^{(2)}$: $O(N^0)$

In the above steps, $\mu$ and $\nu$ refer to atomic orbitals, $P$ refers to both RAS I and RAS III orbitals, and $p,q,r$, and $s$ refer to RAS II orbitals. $\mathbf{D}_X$ is a vector of the denominators. The hat on $J$ and $K$ indicates that only the RAS I density matrix was used in the integral digestion. Note that even though the two-electron integrals are stored in memory, the memory demands are quite minimal as there are only $O(N^0)$ and $O(N^1)$ of the $(pq|rs)$ and $(Pq|rs)$ integrals, respectively. The memory requirements are thus quadratic owing to the $\hat{J}_{\mu\nu}$ and $\hat{K}_{\mu\nu}$ matrices. For small number of spin-flips, the overall bottleneck is the formation of the integrals which scales as $O(N^3)$. The Armadillo C++ Linear Algebra package was used to facilitate the implementation.[58] The resolution-of-the-identity approximation (RI) was used in computing the two-electron integrals, providing a significant computational speed-up with negligible error.[59,60]

Comparing the relative costs of the RAS-$n$SF and SF-CAS(h,p)$_n$ methods, it is easily seen that the cost of either possible bottleneck (integrals or CI) is going to be reduced for the new methods. In RAS-$n$SF, the particle (and hole) states are directly coupled, so integrals with two virtual and two active indices, $\langle VA||VA\rangle$, are needed, which increases the scaling to $O(N^4)$, compared to $O(N^3)$ for SF-CAS(h,p)$_n$. For large active spaces and solving for many states, the CI component can easily become the bottleneck in a RAS-$n$SF calculation. SF-CAS(h,p)$_n$ simplifies this by replacing the iterative $O(N^2)$ $\sigma$-vector evaluation with a noniterative $O(N^1)$ matrix multiply.

## III. NUMERICAL TESTS

The performance of the target RAS-$n$SF results has been investigated in previous papers[25−28,61,62] and has been found to provide qualitatively accurate results for a wide range of molecules. The SF-CAS(h,p)$_n$ methods are approximations to the fully variational RAS-$n$SF method, and thus we aim to evaluate the quality of this approximation in a well-defined manner, by direct comparison to RAS-$n$SF results. A variety of computed quantities are used in this evaluation, including spin-state energy gaps, potential energy surface scans, and excited state profiles.

All calculations have been performed with a development version of Q-Chem 4.0.[63] Cartesian coordinates can be obtained in the Supporting Information for all systems. Molecular orbital isosurfaces have been rendered using the IQmol software.[64]

**A. Spin-State Energy Gaps.** Organic radicals have enjoyed a great amount of interest due to their potential application to organic magnetic and conducting materials.[65] Crystals or polymers built from molecular building blocks which contain unpaired electrons have the potential for exhibiting emergent bulk magnetic or conductive properties. The realization of this largely depends on the underlying stability of the radicals and the manner in which the radical units couple.

One of the more attractive features of the RAS-$n$SF method is the reliability with which ground state spin multiplicity can be predicted, even for extremely small energy gaps.[28] In this section, we assess the accuracy of the SF-CAS(h,p)$_n$ approximation for computing the relative energies of spin states, using 68 different energy gaps between singlet, triplet, and quintet spin states. In Figure 2a, we plot the perturbative results, sans level shift, against the fully variational RAS-$n$SF energy gaps. In Figure 2b, the results are shown after choosing a level-shift value which minimizes the RMS. This optimal value, $\eta$, is given in Table 1.

All geometries were optimized at the B3LYP/6-31g* level for the high-spin state and are provided in the Supporting Information. Vertical spin-state energy gaps are computed using single point calculations either at the SF-CAS(h,p)$_n$/6-31g* level or the RAS-$n$SF/6-31g* level.


dx.doi.org/10.1021/ct400898p | J. Chem. Theory Comput. 2014, 10, 589−599

**Table 1. Errors in Spin-State Energy Gaps MAD (MAX) Errors (Units in kcal/mol)**

| MAD (MAX), kcal/mol | $\eta$ = 0 | $\eta$ = opt | $\eta$, mH |
|---|---|---|---|
| SF-CAS | 2.14(−10.0) | 2.14(−10.0) | |
| SF-CAS(h,p) | 0.29(−1.3) | 0.28(1.12) | −16 |
| SF-CAS(h,p)$_0$ | 1.34(7.4) | 0.24(1.57) | 116 |
| SF-CAS(h,p)$_1$ | 1.09(5.0) | 0.22(1.58) | 107 |

*Without Level Shift.* In Figure 2a, both the zeroth-order SF-CAS and the second-order SF-CAS(h,p)$_n$ qualitatively reproduce the RAS-*n*SF results. Neglecting all hole and particle relaxation, the SF-CAS energy gaps (high-spin minus low-spin) are consistently underestimated. This is to be expected as the orbitals have been optimized for the high spin state (either triplet or quintet in this data) and not the low-spin states.

After inclusion of the perturbative correction describing hole and particle relaxation, the energy gaps increase, owing to a relaxation of the low-spin states. For the nondegenerate perturbation theory (NDPT) results, SF-CAS(h,p) (depicted as blue squares) performs surprisingly well with a MAD from the RAS-*n*SF results of only 0.29 kcal/mol.

However, when the theory is made more sophisticated by moving to a quasidegenerate perturbation theory (QDPT), the SF-CAS(h,p)$_n$ results become noticeably worse. This can be understood as a partial cancellation of two different errors in the NDPT results. The perturbative coefficients of the hole and particle determinants, and thus the energy corrections, are overestimated by second-order perturbation theory. However, for the NDPT, the zeroth-order SF-CAS-CI eigenvectors do not diagonalize the effective Hamiltonian (see eq 13), and thus the energy is necessarily higher than the ground state of the effective Hamiltonian. These two opposing effects work to cancel errors for the NDPT SF-CAS(h,p) results. When QDPT is used, the effective Hamiltonian stays essentially the same with the same overestimated corrections but now is diagonalized to yield even larger corrections. This effect translates into spin state energy gaps which are too large, since only the low-spin states are corrected by the perturbation.[83] While this might urge one to advocate only for the nondegenerate SF-CAS(h,p) method, this error cancellation might not always occur. Furthermore, the NDPT correction will no longer be well-defined when actual quasidegeneracies occur (see section III.D). Therefore, analysis of the QDPT results reveals deficiencies of the effective Hamiltonian that would have gone unnoticed if only the NDPT results were considered.

*With Level Shift.* As seen in the overestimation of the energy gaps, the first-order hole and particle coefficients are found to be systematically overestimated. To correct this, we have repartitioned the Hamiltonian using a level shift which effectively pads the energy of the perturbing states to protect against small denominators. As described in eq 8, this is equivalent to diagonalizing the unfolded second-order Hamiltonian, with a penalty function that damps large external space amplitudes. The value of this level shift, however, must be determined empirically. For this work, we chose values which made the SF-CAS(h,p)$_n$ results most similar to the RAS-*n*SF results as quantified by the RMS deviation. The optimal values for these data were found to be 107 mH and 116 mH for SF-CAS(h,p)$_0$ and SF-CAS(h,p)$_1$, respectively. Because the NDPT SF-CAS(h,p) underestimated the gaps, the level-shift parameter optimized to a negative value of −16 mH. After optimizing $\eta$, all three perturbative theories perform similarly with results that fall directly in line with the RAS-*n*SF data, as seen in Figure 2b.

The level shift does not simply decrease the size of all perturbative corrections as a multiplicative scale factor would. Energy gaps which were accurate without a level shift are minimally affected, while the few energy gaps with significant errors are improved drastically. The padding of the denominator thus lends a degree of stability to the SF-CAS(h,p)$_n$ theories, which justifies the slight empiricism.

**B. HF Potential Energy Surface.** The diatomic molecule HF provides a challenging test case for computing bond dissociation energies, having both a strong bond energy ($D_0$ = 135.1 kcal/mol)[66] and a challenging electronic structure. The lone pairs on the F atom interact non-negligibly with the bond at equilibrium distances, and at dissociation all three p orbitals on F become equivalent. Therefore, as was done previously using RAS-*n*SF,[28] the active space is (six electrons, four orbitals) and was chosen to contain the four orbitals which dissociate to 2p$_{x,y,z}$ on F and 1s on H. As degeneracy among multiple triplet states can occur when an open-shell configuration is very unstable (i.e., near equilibrium position), care must be taken to ensure that the appropriate triplet state, $|\sigma(\alpha)\sigma^*(\alpha)\rangle$, is obtained to properly model the dissociative process.[19] Calculations on the HF molecule employed the aug-cc-pVTZ basis set.[67]

In Figure 3, the PES of HF is presented. Here, the RAS-*n*SF (shown as boundary of gray area) is compared to the zeroth-order SF-CAS, the nondegenerate SF-CAS(h,p) method, and the various SF-CAS(h,p)$_{0,1,\infty}$ quasidegenerate methods. All four perturbative methods reproduce the qualitative energy lowering and $R_0$ shift observed when including the particle and hole states.

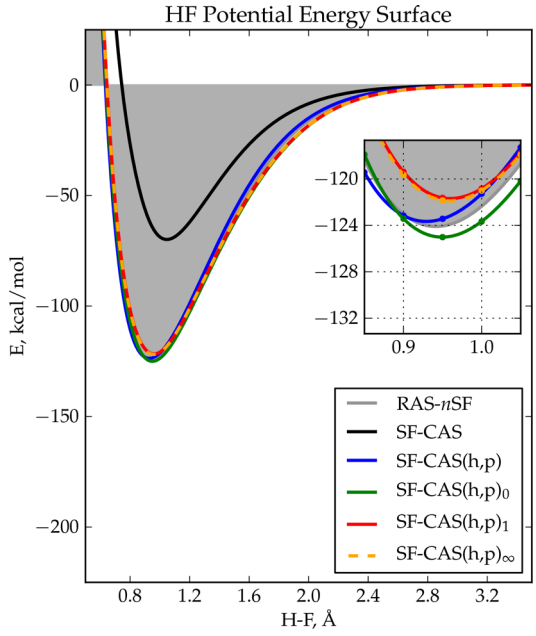


**Figure 3.** HF bond dissociation curves. (6,4) active space and triplet reference. Gray area: RAS-*n*SF. Black curve: SF-CAS. Blue curve: SF-CAS(h,p). Green curve: SF-CAS(h,p)$_0$. Red curve: SF-CAS(h,p)$_1$. Orange dotted line: SF-CAS(h,p)$_\infty$. *y* axis is in units of kcal/mol and same scale in both plots. *x* axis in units of Å. Optimal level shifts employed.

Inclusion of the SF-CAS(h,p)$_\infty$ results (shown as orange dotted line) provides a reference for evaluating the accuracy in truncating the binomial expansion in eq 19. Comparing the SF-


dx.doi.org/10.1021/ct400898p | J. Chem. Theory Comput. 2014, 10, 589−599

CAS(h,p)$_0$ and SF-CAS(h,p)$_\infty$ curves, it is observed that the truncation of the binomial expansion at zeroth order leads to an overestimation of the correction. By including the linear term in eq 19, the SF-CAS(h,p)$_1$ method provides virtually identical results to SF-CAS(h,p)$_\infty$. This suggests that any error introduced by removing the state dependence from the effective Hamiltonian is negligible for the SF-CAS(h,p)$_1$. For this system, the NDPT correction also provides an accurate approximation to the RAS-*n*SF curve, although slightly overestimating the minimum.[84]

Overall, the SF-CAS(h,p)$_n$ methods are able to accurately model the active-space relaxation effects that are accounted for variationally in RAS-*n*SF. Referenced to SF-CAS(h,p)$_\infty$, SF-CAS(h,p)$_1$ provides a dramatic improvement over SF-CAS-(h,p)$_0$.

**C. $N_2$ Potential Energy Surface.** Dissociation of the triply bonded nitrogen molecule requires the computation of the potential energy surface between a closed-shell singlet at equilibrium and two singlet-coupled quartet N atoms. Single reference wave functions are inadequate to model this surface, and multireference approaches like CASSCF are often needed. Alternatively, in a spin-flip framework, one can obtain a qualitatively correct description of the PES starting from a single determinant wave function (the high-spin heptet). The RAS-*n*SF method was shown to yield an $N_2$ PES of comparable accuracy to CASSCF,[27] which clearly highlights the ability of the hole and particle excitations to describe the orbital relaxation effects of the active space configurations. In Figure 4, the PES of $N_2$ is presented, comparing the SF-CAS, SF-CAS(h,p), SF-CAS(h,p)$_0$, and SF-CAS(h,p)$_1$ methods to the RAS-*n*SF results. Calculations were carried out using the cc-pVDZ basis set and used the (6,6) *natural* active space (the minimal active space which allows the desired number of spin-flips).[67]

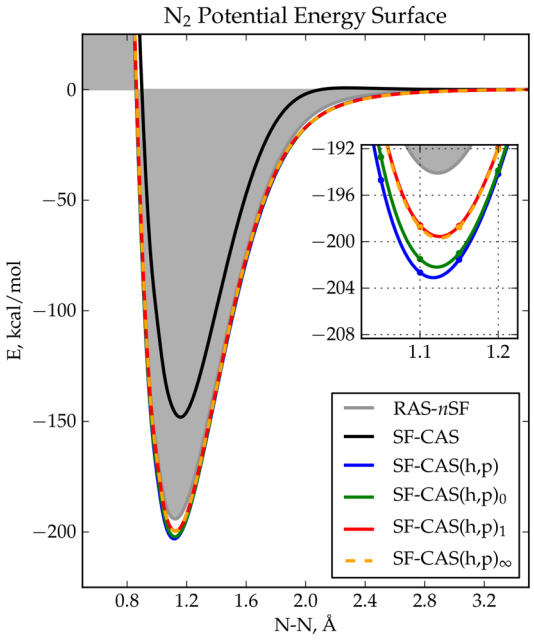


**Figure 4.** $N_2$ Bond dissociation curves. (6,6) active space and heptet reference. Gray area: RAS-*n*SF. Black curve: SF-CAS. Blue curve: SF-CAS(h,p). Green curve: SF-CAS(h,p)$_0$. Red curve: SF-CAS(h,p)$_1$. Orange dotted line: SF-CAS(h,p)$_\infty$. *y* axis is in units of kcal/mol and same scale in both plots. *x* axis in units of Å. Optimal level shifts employed.

A prerequisite for perturbation theory is that the zeroth-order wave function is at least qualitatively correct. Here, SF-CAS does provide a decent description of the bond dissociation, recovering almost 150 kcal/mol of the binding energy. By including the perturbative hole and particle corrections, comparison to the RAS-*n*SF curve is significantly enhanced, with the SF-CAS(h,p)$_1$ and SF-CAS(h,p)$_\infty$ curves lying roughly 5 kcal/mol (3% error) lower in energy. The SF-CAS(h,p)$_0$ curve overshoots by an additional 3 kcal/mol, a clear impact of the approximate denominator in eq 19.

One interesting feature of this plot is the slight barrier on the SF-CAS curve around 2.2 Å. Here, the SF-CAS energy rises above the energy of the separated N atoms, a result of orbital mixing between the active space orbitals and the nonbonding lone pairs. Interestingly, all perturbative corrections are unaffected by this, providing accurate energies all along the PES.

**D. Electronic Transitions in Biradical Porphyrin Complex.** Establishing reliable microscopic control over molecular properties such as conductance and magnetism has been an ongoing effort for the past several years. While technological applications will ultimately require the manipulation of difficult to compute properties, such as magnetic anisotropy, the reliable prediction of ground state spin multiplicity is still out of reach for standard quantum chemical approaches. One class of molecules which carries a great deal of potential for molecular devices is that for which the magnetic properties can be manipulated with light.[68]

One interesting example can be found in ref 69, wherein a metalated porphyrin ring with a ligated organic radical can transition from a very weakly antiferromagnetic ground state to a ferromagnetic excited state. In this example, Cu(II) (**M**) occupies the center of the porphyrin ring[85] (**P**) and possesses an unpaired electron. Attached to one of the porphyrin's pyrrole rings is an organic $\pi$-radical (verdazyl or **Vz**).[70−73] In the ground state, $|\dot{\mathbf{M}}{-}\mathbf{P}{-}\dot{\mathbf{V}}\mathbf{z}\rangle$, these unpaired electrons are very weakly coupled ($J \approx 5{-}10$ cm$^{-1}$), due to the radical−radical distance and the perpendicular orientation of the **Vz** ring to **P**. However, upon irradiation, a local triplet state can be created on *P* which can mediate long-range spin-coupling between the **M** site and **Vz**, i.e., $|\dot{\mathbf{M}}{-}\ddot{\mathbf{P}}{-}\dot{\mathbf{V}}\mathbf{z}\rangle$. This is illustrated schematically in Figure 5.

To study only the $|\dot{\mathbf{M}}{-}\mathbf{P}{-}\dot{\mathbf{V}}\mathbf{z}\rangle$ ground state, a single spin-flip starting from a triplet reference is sufficient. RAS-1SF and all the SF-CAS(h,p)$_n$ methods predict very similar results for the singlet−triplet splitting of ∼0.1−0.2 meV. Although, all the spin-flip calculations predict the triplet to lie slightly lower in energy than the singlet, which is at odds with the experimental conclusions, the fact that the states are nearly degenerate and that both will be populated in experiment is clearly reproduced here. One possible source for this discrepancy could be that we are using a rather insufficient basis set (6-31G) for these calculations. However, for the sake of evaluating the current approximation, the SF-CAS(h,p)$_n$ methods all agree very closely with the RAS-SF results.

To model the $|\dot{\mathbf{M}}{-}\ddot{\mathbf{P}}{-}\dot{\mathbf{V}}\mathbf{z}\rangle$ excited state, four electrons clearly need to be correlated. While a double spin-flip calculation is often sufficient for treating four spin-coupled electrons, porphyrins have a well-understood electronic structure which is largely described by the Gouterman four-orbital model,[74−77] in which electrons in two nearly degenerate $a_{1u}$ and $a_{2u}$ orbitals can be excited into a doubly degenerate $e_g$ orbital. In order to correctly correlate the four electrons while maintaining a proper description of the **P** electronic structure, triple spin-flip


dx.doi.org/10.1021/ct400898p | J. Chem. Theory Comput. 2014, 10, 589−599

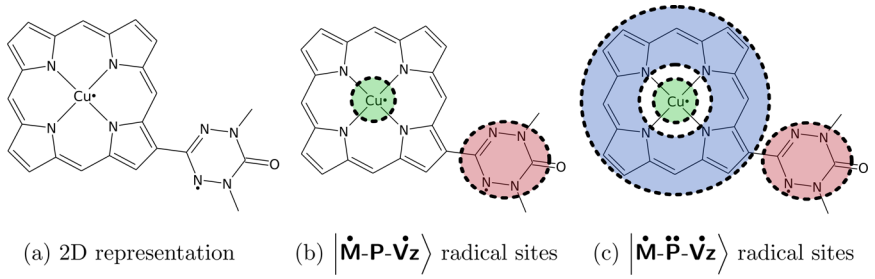


**Figure 5.** (a) Chemical structure for the Cu(II) porphyrin derivatized with a verdazyl group. (b) Schematic description of radical sites in the ground state. (c) Schematic description of radical sites in the excited state.

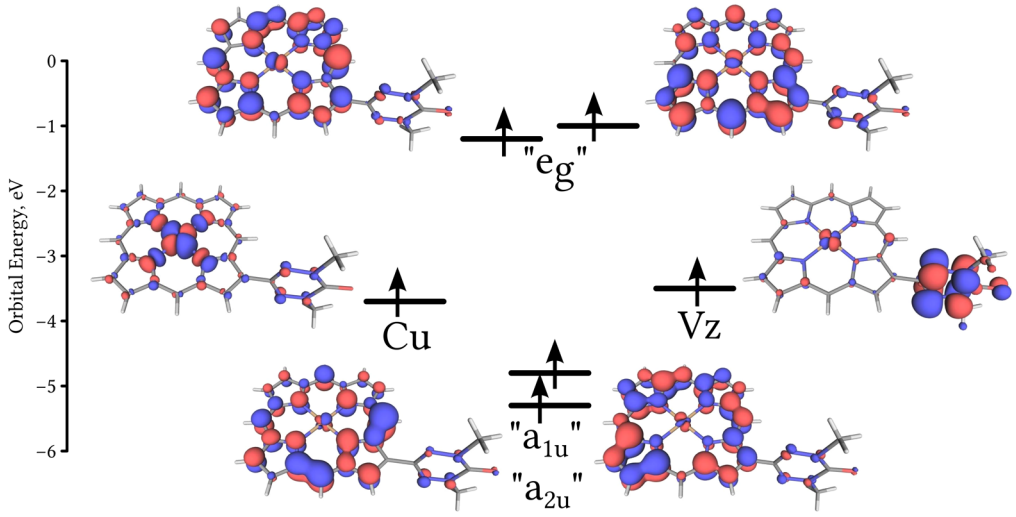


**Figure 6.** Molecular orbitals constituting the active space for the heptet ROHF reference. The active space contains the **M** and **Vz** singly occupied orbitals and the porphyrin-based orbitals which correspond to the $a_{1u}$, $a_{2u}$, and $e_g$ orbitals of the traditional four-orbital model for porphyrins.

calculations were performed using the heptet ROHF orbitals, which are shown in Figure 6.

The resulting low-energy spectrum is comprised of a nearly degenerate pair of singlet and triplet $|\dot{\mathbf{M}}{-}\mathbf{P}{-}\dot{\mathbf{V}}\mathbf{z}\rangle$ states, with a higher lying group of four $|\dot{\mathbf{M}}{-}\ddot{\mathbf{P}}{-}\dot{\mathbf{V}}\mathbf{z}\rangle$ states at around 2.3 eV. These four states are made up of one quintet, two triplets, and one singlet. The excitation energies for the $|\dot{\mathbf{M}}{-}\ddot{\mathbf{P}}{-}\dot{\mathbf{V}}\mathbf{z}\rangle$ states are shown in the top of Figure 7 for the SF-CAS, SF-CAS(h,p), SF-CAS(h,p)$_0$, SF-CAS(h,p)$_1$, and RAS-SF methods, respectively.

The SF-CAS energies significantly underestimate the excitation energy. This is a direct result of the absence of low-spin orbital relaxation effects, which are, not surprisingly, more important for the $|\dot{\mathbf{M}}{-}\mathbf{P}{-}\dot{\mathbf{V}}\mathbf{z}\rangle$ states than the $|\dot{\mathbf{M}}{-}\ddot{\mathbf{P}}{-}\dot{\mathbf{V}}\mathbf{z}\rangle$ states. The SF-CAS(h,p) overestimates this effect, and the resulting excitation energies are too large. The results are significantly improved by using the quasidegenerate theories SF-CAS(h,p)$_0$ and SF-CAS(h,p)$_1$, with the latter providing the best comparison to the RAS-SF excitation energies.

While getting accurate excitation energies is, of course, important, perhaps equally interesting is the extent to which the new models can reproduce the RAS-SF spin-state splittings in the $|\dot{\mathbf{M}}{-}\ddot{\mathbf{P}}{-}\dot{\mathbf{V}}\mathbf{z}\rangle$ excited state. Consistent with experimental results, each method predicts an increased spin-state splitting in the excited state, with the quintet state being the most stable. Although each method predicted the correct ordering of spin states (low to high energy: quintet, triplet, triplet, singlet), quantitatively reproducing the relative spin-state splittings appears to be more difficult. To quantify the homogeneity of the spin-state splittings for the different methods, we take the average of the first and last gap and divide this by the second gap

$$x = \frac{(E_{T1} - E_Q + E_S - E_{T2})}{2E_{T2} - 2E_{T1}} \tag{26}$$

This is plotted in the bottom of Figure 7 for each of the methods.

Looking first at the zeroth-order method, SF-CAS, we see a much less homogeneous energy spread compared to RAS-SF. Using the NDPT does not improve this at all, and the SF-CAS(h,p) method has very similar state splittings to those of SF-CAS. QDPT, however, does improve the energy splittings with the SF-CAS(h,p)$_1$ model providing the best results of the perturbative methods.

To illustrate the efficiency advantages, Table 2 lists the wall times on a single CPU for the reported calculations.[86] Note that these timings should be interpreted lightly as they are obtained by comparison to a spin-adapted, exact integral implementation of RAS-*n*SF, while our implementation is determinant-driven and uses RI integrals.

## IV. CONCLUSIONS

In this paper, we have reported on the development and testing of a new spin-flip method termed SF-CAS(h,p)$_n$. This is a quasidegenerate perturbative approximation to the restricted active space spin-flip CI method (RAS-SF), which provides significant computational efficiency gains, while introducing only modest errors. Three different methods were discussed in this paper, namely SF-CAS(h,p), SF-CAS(h,p)$_0$, and SF-CAS(h,p)$_1$.


dx.doi.org/10.1021/ct400898p | J. Chem. Theory Comput. 2014, 10, 589−599

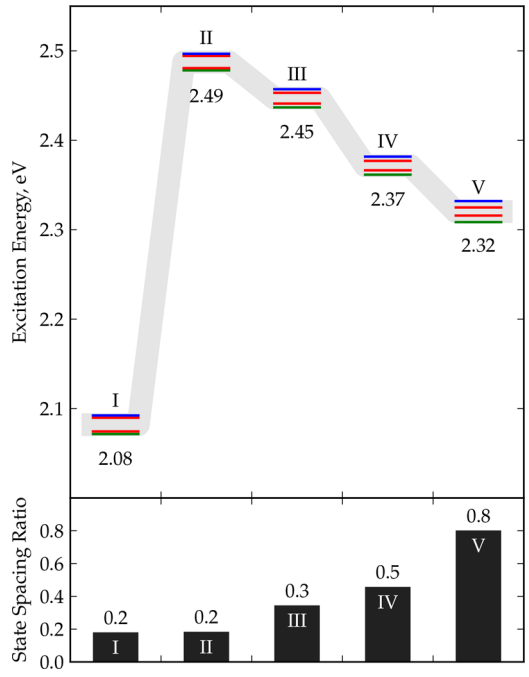


**Figure 7.** (Top) $|\dot{M}-P-\dot{V}z\rangle \rightarrow |\dot{M}-\ddot{P}-\dot{V}z\rangle$ excitation energies. Data labels refer to the average of the spin-state energies. Blue (singlet). Red (triplet). Green (quintet). (Bottom) Homogeneity of the spin-state energy splitting in the $|\dot{M}-\ddot{P}-\dot{V}z\rangle$ state. Energies relative to the ground electronic state. Roman numerals denote which theory was used: (I) SF-CAS. (II) SF-CAS(h,p). (III) SF-CAS(h,p)$_0$. (IV) SF-CAS(h,p)$_1$. (V) RAS-SF. Same level-shift parameters used as above.

**Table 2. Timings for Running the Porphyrin System on a Single CPU Core**[a]

| | RAS-SF | SF-CAS(h,p) | SF-CAS(h,p)$_0$ | SF-CAS(h,p)$_1$ |
|---|---|---|---|---|
| time (s) | 7479.392 | 52.348 | 53.552 | 61.028 |
| relative | 100.00% | 0.70% | 0.72% | 0.82% |

[a]SCF times are neglected from comparison. Times are given in seconds. Six RAS-SF states were converged for the singlet, triplet, and quintet multiplicities.

Of these, the most interesting is the SF-CAS(h,p)$_1$ theory as it is both quasidegenerate and also a very good approximation to the iterative and single-state SF-CAS(h,p)$_\infty$ theory.

The current method retains the core theoretical features of RAS-SF such as spin-purity, size-consistency, and orbital invariance, while losing variationality. Relative to RAS-SF, its primary limitation is the inability to describe excited states whose zero order description includes significant contributions from either particle or hole configurations. This is typically not the case for low-lying excited states of strongly correlated molecules, treated with a number of spin flips that is half the number of strongly correlated electrons.

We have tested the current method on a set of 68 spin-state energy gaps, for organic polyradicals. From these data, we found the SF-CAS and SF-CAS(h,p) methods to underestimate high-spin minus low-spin gaps, while the quasidegenerate methods overestimated the gap. To stabilize the perturbative correction, we used a single level-shift parameter to damp large perturbative amplitudes. The value of this level shift was optimized by minimizing the root mean squared deviation to the RAS-nSF results. Although the diversity of the data set used for the optimization is not quite ideal, the optimal values of the SF-CAS(h,p)$_0$ and SF-CAS(h,p)$_1$ methods (116 mH and 107 mH, respectively) appear to be reasonably transferable based on our extension to remaining test cases throughout the paper. Contrary to the QDPT methods, the level shift for the SF-CAS(h,p) method optimized to a negative number (−16 mH). The stabilizing effect of the level shift only makes sense for positive level shifts, so we do not recommend any level shifting with the SF-CAS(h,p) method.

Using the optimized level-shift values, bond dissociation curves were computed for $N_2$ and FH molecules. Good agreement was found between the perturbative curves and the variational curves.

To highlight the computational advantages of the current approach, a large biradical porphyrin system was investigated. Here, SF-CAS(h,p)$_1$ provided significant improvements over SF-CAS and the other PT methods, in both excitation energy and excited state spin-state splittings. For this system, the perturbative approximation was two orders of magnitude faster than the variational RAS-SF computation.

We anticipate the SF-CAS(h,p)$_1$ model to stand as both an economical alternative to the RAS-*n*SF method and a foundation for further developments incorporating dynamical correlation effects.

## ■ ASSOCIATED CONTENT

### Supporting Information

All xyz coordinates of the molecules studied in the paper are included. This information is available free of charge via the Internet at http://pubs.acs.org/.

## ■ AUTHOR INFORMATION

### Corresponding Author

*E-mail: mhg@cchem.berkeley.edu.

### Notes

The authors declare no competing financial interest.

## ■ ACKNOWLEDGMENTS

Support for this work was provided through the Scientific Discovery through Advanced Computing (SciDAC) program funded by the U.S. Department of Energy, Office of Science, Advanced Scientific Computing Research, and Basic Energy Sciences. We are grateful to Khalid Ibrahim and Sam Williams for helpful discussions concerning the design of the software. Additionally, we would like to thank David Stück, Dr. Fran Bell, and Dr. Paul Zimmermann for insightful discussions related to this work.

## ■ REFERENCES

(1) Møller, C.; Plesset, M. S. *Phys. Rev.* **1934**, *46*, 618−622.
(2) Paldus, J.; Shavitt, I.; Čižek, J. *Phys. Rev. A* **1972**, *5*, 50.
(3) Čižek, J. *J. Chem. Phys.* **1966**, *45*, 4256.
(4) Coester, F.; Kümmel, H. *Nucl. Phys.* **1960**, *17*, 477−485.
(5) Roos, B. O. *Int. J. Quantum Chem.* **1980**, *18*, 175−189.
(6) Chan, G. K.-L.; Zgid, D. The Density Matrix Renormalization Group in Quantum Chemistry. In *Annual Reports in Computational Chemistry*; Elsevier: Amsterdam, 2009; Chapter 7, pp 149−162.
(7) Neuscamman, E. *Phys. Rev. Lett.* **2012**, *109*, 203001.
(8) Mazziotti, D. *Phys. Rev. Lett.* **2006**, *97*, 143002.
(9) Parkhill, J. A.; Head-Gordon, M. *J. Chem. Phys.* **2010**, *133*, 124102.
(10) Parkhill, J. A.; Lawler, K.; Head-Gordon, M. *J. Chem. Phys.* **2009**, *130*, 084101.
(11) Small, D. W.; Head-Gordon, M. *J. Chem. Phys.* **2012**, *137*, 114103.
(12) White, S. R. *Phys. Rev. B* **1993**, *48*, 10345−10356.
(13) White, S. R. *Phys. Rev. Lett.* **1992**, *69*, 2863−2866.

(14) Roos, B. O.; Andersson, K.; Fülscher, M. P. *Chem. Phys. Lett.* **1992**, *192*, 5−13.
(15) Shao, Y.; Head-Gordon, M.; Krylov, A. I. *J. Chem. Phys.* **2003**, *118*, 4807.
(16) Krylov, A. *Chem. Phys. Lett.* **2001**, *350*, 522−530.
(17) Krylov, A. I.; Sherrill, C. D. *J. Chem. Phys.* **2002**, *116*, 3194.
(18) Krylov, A. I. *Chem. Phys. Lett.* **2001**, *338*, 375−384.
(19) Krylov, A. I.; Sherrill, C. D. *J. Chem. Phys.* **2002**, *116*, 3194.
(20) Levchenko, S. V.; Krylov, A. I. *J. Chem. Phys.* **2004**, *120*, 175−85.
(21) Bernard, Y. A.; Shao, Y.; Krylov, A. I. *J. Chem. Phys.* **2012**, *136*, 204103.
(22) Xu, X.; Gozem, S.; Olivucci, M.; Truhlar, D. G. *J. Phys. Chem. Lett.* **2012**, 253−258.
(23) Zhekova, H.; Seth, M.; Ziegler, T. *J. Chem. Theory Comput.* **2011**, *7*, 1858−1866.
(24) Sears, J. S.; Sherrill, C. D.; Krylov, A. I. *J. Chem. Phys.* **2003**, *118*, 9084.
(25) Casanova, D.; Head-Gordon, M. *J. Chem. Phys.* **2008**, *129*, 064104.
(26) Zimmerman, P. M.; Bell, F.; Goldey, M.; Bell, A. T.; Head-Gordon, M. *J. Chem. Phys.* **2012**, *137*, 164110.
(27) Bell, F.; Zimmerman, P.; Casanova, D.; Goldey, M.; Head-Gordon, M. *Phys. Chem. Chem. Phys.* **2012**, *15*, 358−366.
(28) Casanova, D.; Head-Gordon, M. *Phys. Chem. Chem. Phys.* **2009**, *11*, 9779−90.
(29) Löwdin, P.-O. *J. Mol. Spectrosc.* **1963**, *10*, 12−33.
(30) Löwdin, P.-O. *J. Math. Phys. (Melville, NY, U. S.)* **1962**, *3*, 969.
(31) Löwdin, P.-O. *J. Chem. Phys.* **1951**, *19*, 1396.
(32) Gershgorn, Z.; Shavitt, I. *Int. J. Quantum Chem.* **1968**, *2*, 751−759.
(33) Li Manni, G.; Ma, D.; Aquilante, F.; Olsen, J.; Gagliardi, L. *J. Chem. Theory Comput.* **2013**, *9*, 3375−3384.
(34) Li Manni, G.; Aquilante, F.; Gagliardi, L. *J. Chem. Phys.* **2011**, *134*, 034114.
(35) Suaud, N.; Ruamps, R.; Guihéry, N.; Malrieu, J.-P. *J. Chem. Theory Comput.* **2012**, *8*, 4127−4137.
(36) Head-Gordon, M.; Oumi, M.; Maurice, D. *Mol. Phys.* **1999**, *96*, 593−602.
(37) Rhee, Y. M.; Casanova, D.; Head-Gordon, M. *J. Chem. Theory Comput.* **2009**, *5*, 1224−1236.
(38) Casanova, D.; Rhee, Y. M.; Head-Gordon, M. *J. Chem. Phys.* **2008**, *128*, 164106.
(39) Miralles, J.; Daudey, J.-P.; Caballol, R. *Chem. Phys. Lett.* **1992**, *198*, 555−562.
(40) Miralles, J.; Castell, O.; Caballol, R.; Malrieu, J.-P. *Chem. Phys.* **1993**, *172*, 33−43.
(41) Calzado, C. J.; Cabrero, J.; Malrieu, J. P.; Caballol, R. *J. Chem. Phys.* **2002**, *116*, 3985.
(42) Calzado, C. J.; Cabrero, J.; Malrieu, J. P.; Caballol, R. *J. Chem. Phys.* **2002**, *116*, 2728.
(43) Barone, V.; Cacelli, I.; Ferretti, A.; Monti, S.; Prampolini, G. *J. Chem. Theory Comput.* **2011**, *7*, 699−706.
(44) Barone, V.; Cacelli, I.; Ferretti, A.; Monti, S.; Prampolini, G. *Phys. Chem. Chem. Phys.* **2011**, *13*, 4709−14.
(45) Barone, V.; Boilleau, C.; Cacelli, I.; Ferretti, A.; Monti, S.; Prampolini, G. *J. Chem. Theory Comput.* **2012**, *9*, 300−307.
(46) Barone, V.; Cacelli, I.; Ferretti, A.; Prampolini, G. *J. Chem. Phys.* **2009**, *131*, 224103.
(47) Kozlowski, P. M.; Davidson, E. R. *J. Chem. Phys.* **1994**, *100*, 3672.
(48) Kozlowski, P.; Davidson, E. *Chem. Phys. Lett.* **1994**, *226*, 440−446.
(49) Davidson, E. *Chem. Phys. Lett.* **1995**, *241*, 432−437.
(50) Murray, C.; Davidson, E. R. *Chem. Phys. Lett.* **1991**, *187*, 451−454.
(51) Glaesemann, K. R.; Schmidt, M. W. *J. Phys. Chem. A* **2010**, *114*, 8772−7.
(52) Crawford, T. D.; Schaefer, H. F.; Lee, T. J. *J. Chem. Phys.* **1996**, *105*, 1060.
(53) Murray, C. W.; Handy, N. C. *J. Chem. Phys.* **1992**, *97*, 6509.
(54) Lauderdale, W. J.; Stanton, J. F.; Gauss, J.; Watts, J. D.; Bartlett, R. J. *Chem. Phys. Lett.* **1991**, *187*, 21−28.
(55) Hubač, I.; Čársky, P. *Phys. Rev. A* **1980**, *22*, 2392−2399.
(56) Ivanic, J.; Ruedenberg, K. *Theor. Chem. Acc.* **2001**, *106*, 339−351.
(57) OpenMP Architecture Review Board. OpenMP Application Program Interface Version 3.0, 2008. http://www.openmp.org.
(58) Sanderson, C. *Matrix* **2010**, 1−16.
(59) Feyereisen, M.; Fitzgerald, G.; Komornicki, A. *Chem. Phys. Lett.* **1993**, *208*, 359−363.
(60) Vahtras, O.; Almlöf, J.; Feyereisen, M. *Chem. Phys. Lett.* **1993**, *213*, 514−518.
(61) Zimmerman, P. M.; Bell, F.; Casanova, D.; Head-Gordon, M. *J. Am. Chem. Soc.* **2011**, *133*, 19944−52.
(62) Casanova, D. *J. Chem. Phys.* **2012**, *137*, 084105.
(63) Shao, Y.; et al. *Phys. Chem. Chem. Phys.* **2006**, *8*, 3172−91.
(64) Gilbert, A. T. B. IQmol Molecular Viewer. http://iqmol.org.
(65) *Magnetic Properties of Organic Materials*; Lahti, P. M., Ed.; Marcel Dekker: New York, 1999.
(66) Johns, J. W. C.; Barrow, R. F. *Proc. R. Soc. London* **1959**, *251*, 504−518.
(67) Dunning, T. H. *J. Chem. Phys.* **1989**, *90*, 1007−1023.
(68) Sato, O.; Iyoda, T.; Fujishima, A.; Hashimoto, K. *Science* **1996**, *272*, 704−705.
(69) Poddutoori, P. K.; Pilkington, M.; Alberola, A.; Polo, V.; Warren, J. E.; van der Est, A. *Inorg. Chem.* **2010**, *49*, 3516−24.
(70) Thompson, L.; Koivisto, B. D.; Hicks, R. G. *Coord. Chem. Rev.* **2005**, *249*, 2612−2630.
(71) Azuma, N. *J. Chem. Phys.* **1974**, *61*, 2294.
(72) McKinnon, S. D. J.; Patrick, B. O.; Lever, A. B. P.; Hicks, R. G. *Chem. Commun.* **2010**, *46*, 773−5.
(73) McKinnon, S. D. J.; Gilroy, J. B.; McDonald, R.; Patrick, B. O.; Hicks, R. G. *J. Mater. Chem.* **2011**, *21*, 1523.
(74) Gouterman, M. *J. Mol. Spectrosc.* **1961**, *6*, 138−163.
(75) Gouterman, M.; Wagnière, G. H.; Snyder, L. C. *J. Mol. Spectrosc.* **1963**, *11*, 108−127.
(76) Ake, R. L.; Gouterman, M. *Theor. Chim. Acta* **1969**, *15*, 20−42.
(77) Gouterman, M. *J. Chem. Phys.* **1970**, *52*, 3795.
(78) Huron, B.; Malrieu, J. P.; Rancurel, P. *J. Chem. Phys.* **1973**, *58*, 5745.
(79) Head-Gordon, M.; Rico, R. J.; Oumi, M.; Lee, T. J. *Chem. Phys. Lett.* **1994**, *219*, 21−29.
(80) Malmqvist, P.-A. k. *Chem. Phys. Lett.* **1995**, *241*, 429−431.
(81) Deciding what this state should be is not necessarily obvious. A seemingly natural choice would be to take the high-spin HF determinant as the reference since the orbitals have been optimized for this state. However, for situations in which the low-spin state is much lower in energy (i.e., bond equilibrium geometries), the energy of this state will become quite large, making the denominator small and the perturbation unstable. Due to the fact that we are flipping spins, the HF determinant is not longer Aufbau-ordered in the target $m_s$ space. The low-spin Aufbau-ordered determinant could, therefore, provide a better reference state near equilibrium bond distances and thus larger denominators. However, this effectively adds a two electron component to the denominator which ultimately destroys orbital invariance of the energy. Taking the ground state CAS wave function as the reference state provides a natural transition between both closed and open shell scenarios and maintains energy invariance. This is similar to the "Barycentric" partitioning in multireference perturbation theory.[78] It is important to note, that single-electron theories such as CIS(D)[79] do not have this ambiguity, as the three reference states listed above are all exactly the HF determinant.
(82) Davidson and Murray introduced OPT2 to address this issue, though they introduced significant orbital invariance as a result.[50] To correct the orbital invariance problems, a new IOPT theory was developed but failed to be size consistent.[80]
(83) For a minimal active space (i.e., only the singly occupied orbitals), the highest multiplicity state remains unaffected by the perturbation and in fact is simply the ROHF energy (although it is the multideterminantal $m_s = 0$ microstate).
(84) Note that the SF-CAS(h,p) curve lies in between the SF-CAS(h,p)$_0$ and SF-CAS(h,p)$_1$. This is only a result of the level shift, which increases the correction for SF-CAS(h,p) and decreases the

correction for SF-CAS(h,p)$_n$. When $\eta$ = 0, the curves are ordered as would be expected with NDPT lying above the QDPT curve.
(85) The actual molecule is based on a tetraphenyl-porphyrin, but in this study we have removed the phenyl rings to simplify the calculations. A few calculations with the SF-CAS(h,p)$_1$ method were performed to verify that this does not noticeably change the results.
(86) Obtaining a meaningful timing comparison is a bit difficult, as the two codes are implemented through different approaches. The RAS-SF implementation[28] used for this comparison employs spin-adapted configuration state functions and computes the eigenstates via Davidson iterations. Our code directly inverts the effective Hamiltonian and thus obtains all resulting states directly. Furthermore, our code uses the RI approximation for the integral evaluation for further speedups, while computing all matrix elements using slater determinants (not spin-adapted). Thus, the reported timings should be interpreted lightly. For the spin-adapted RAS-SF calculations, six, six, and five states were converged for the singlet, triplet, and quintet multiplicities, respectively. Times reported are averaged over five separate calculations each.